www.czasopisma.pan.pl PAN POLSKA AKADEMIA NAUK www.journals.pan.pl

A R C H I V E S O F M E T A L L U R G Y A N D M A T E R I A L S

Volume 60 2015 Issue 2

DOI: 10.1515/amm-2015-0173

P. BORKOWSKI*,♯, A. SIENICKI*

CONTACTS EROSION MODELLING USING ANSYS COMPUTER SOFTWARE AND EXPERIMENTAL RESEARCH

MODELOWANIE EROZJI STYKÓW Z WYKORZYSTANIEM PROFESJONALNEGO PROGRAMU KOMPUTEROWEGO ANSYS WRAZ Z WERYFIKACJĄ EKSPERYMENTALNĄ

The paper presents a method of contacts' erosion modelling by using computer simulation and analyzing heating, melting and evaporation processes, which cause contact erosion due to application of electric arc. Calculations have been conducted using professional ANSYS software which allows for thermal processes simulation and includes phase transitions for Ag, Cu, W metals and Ag-W50 composite.

Keywords: contacts, electrical arc, mass transfer, contact erosion modelling, ANSYS software

Artykuł przedstawia metody modelowania erozji stykowej z wykorzystaniem symulacji komputerowej i analizy procesów nagrzewania, topnienia i parowania, które powodują erozję styków pod wpływem oddziaływania łuku elektrycznego. Obliczenia zostały przeprowadzone za pomocą profesjonalnego programu komputerowego ANSYS, który pozwala na symulację procesów termicznych z uwzględnieniem przemian fazowych dla styków wykonanych z metali: Ag, Cu, W, a także kompozytów Ag-W50.

1. Introduction

Low-voltage switch users care for the greatest longevity and reliability of those devices. Electric contacts are parts of the switch that are the most vulnerable to exploitation and can lead to switch damage. Knowledge of arc erosion of different contact materials is important for the engineers to be able to choose proper materials for low-voltage switch contacts.

High requirements for contemporary AC low-voltage (LV) switches lead to necessity of using composite materials for the contacts that have specific electric properties and are of high production quality. Those materials should be characterized by high resistance for electric arc erosion, load short-circuit current tacking and should also provide low and stable contact resistance during operation.

In the authors' opinion, computer modelling is far less expensive form of obtaining qualitative and quantitative contact erosion results than conducting experimental research, especially in the field of high currents that occur during short circuit. An attempt to describe theoretically the arc's effect on contacts was undertaken by many scientists in the last 40 years. They created different mathematical models. To solve them, first they used analytical methods. Along with the development of computer technology they started using numerical methods. Research for the currents below 1kA was conducted among others by Kubono [1], Tchalakov and others [2], Lefort and Andanson [3], Lefort and others [4], Bor-Jenq and Nannaji [5], Kharin and others [6], Chabrerie and others [7, 8], Nouri and others [9]. Research for the range of currents above 1 kA was conducted among others by Lefort and others [4], Nahagawa and Yoshioka [10] and Borkowski and others [13-18]. In most of the mentioned cases the calculations focused mainly on the temperature distribution in the contact. The obtained results were presented mainly as isotherms for the anodes and cathodes.

Swingle & McBride [11] were the first to propose a complete model of energy transfer from arc to contacts for low currents. In their erosion mechanism analysis they stated minimal erosion when evaporated material was removed and maximal erosion when not only the evaporated material was removed but also the one that had reached its melting temperature.

The development of this model for low currents was proposed in the paper [12] as a magneto-hydrodynamics model which additionally takes into account arc erosion due to splash erosion. Basing on Swingle & McBride model in the publication [14] there were proposed thermal models of short arc between high-current contacts, with analysis of the amount of energy delivered to electrodes (anode and cathode).

The complexity of physical phenomena and the dynamics of changes in the arc are resulting in difficulties in their mathematical description. Especially it concerns in case of high currents above 1 kA (current half-wave, 50 Hz). Because of that in this paper it was proposed to consider the arc as a "black box" with input and output signals. The input signals are: experimentally measured circuit current and time varying arc voltage. The output signal is time varying arc power received by multiplication of the two formerly mentioned input signals. The amount of power delivered to the contacts will be

* DEPARTMENT OF ELECTRICAL APPARATUS, TECHNICAL UNIVERSITY OF LODZ, B. STEFANOWSKIEGO 18/22, 90-924 ŁÓDŹ, POLAND

♯ Corresponding author: piotr.borkowski@p.lodz.pl

reduced by the power loss due to arc column radiation. Available professional simulation software i.e. ANSYS, enables to adapt such an approach. For such a calculation thermal modules are used. Arc power density, which is calculated from dividing the arc power by the arc root area, is delivered to the contacts.

Having the above in mind, the authors proposed modelling method of electric arc's thermal and erosion effect on contacts using computer simulation and analysis of processes of heating, melting and evaporating of the contacts materials exposed to electric arc. The amount of melted and evaporated contact material along with explosive and plasma ejection of molten metal depends on both amount of arc-generated thermal power and material's thermal properties. Thermal analysis of physical phenomenon in the arc and contacts allows for obtaining temperature distribution in the contacts as well as shape and size of metal's melted part. This allows for further quantitatively estimating theoretical limits of contacts erosion and thus switching durability of a switch while interrupting the current circuit. For the calculations professional ANSYS software was used.

To perform contact erosion modelling basic and specific assumptions need to be defined.

2. Initial (entry) assumptions

Calculations of temperature field distribution in contacts will be conducted with the following basic assumptions:

1. Contacts have shape and size as on Figure 1.
2. Contacts' material – silver, copper and tungsten as well as Ag-W50 consisting of the following volumetric ratio: 50%W / 50%Ag, which corresponds to weight ratio of the composite material W-Ag35 (35.23%Ag / 64.77%W).
3. 3D model for metals and 2D model for composite will be used.
4. In creation of 3D and 2D models, principal of symmetry will be used, which allows for increase in calculations precision.
5. For Ag-W composite calculations, chess-type model structure was adopted (presented on Figure 2) typical for composites made by powder method.
6. Properties of contact material such as enthalpy, density, thermal conductivity and material specific heat are functions of temperature [20-23]. Due to the lack of material data in available literature regarding Ag-W50 composite authors used thermal and physical properties of silver and tungsten for the individual components by modelling the chessboard- type structure.

Additionally, the following simplifying assumptions were defined:

1. Thermal power of the arc is relayed through arc-root to contact surface layer.
2. Joule's heat is omitted.
3. Lateral surface of the electrode has temperature equal to ambient temperature.
4. Thermal exchange with surroundings through convection and radiation was omitted due to very short time of electric arc's duration and contact's low thermal time constant.
5. It was assumed that 80% of arc's power is supplied to contacts and 20% is dispersed to the surroundings [19].

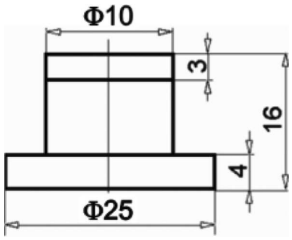

Fig. 1. Test contact

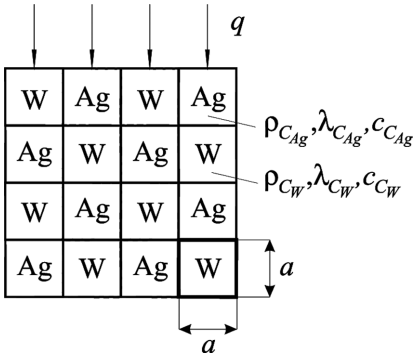

Fig. 2. Ag-W composite structure [18]

6. It was assumed that thermal energy stream led from arc to contact is divided in relation: 50% for cathode and 50% for anode[1)].
7. Practical case of shutting the current off when arc-root's diameter is less than contact's diameter was assumed. For contacts with 10 mm in diameter such situation takes place when shutting the current off while its amplitude is less than 7 kA.
8. Surface power density in spot replacements will be considered, because at the present state of knowledge on elementary and partial spots it is impossible to define their arrangement on contacts surface.
9. Movement of the arc root on the contacts during the disconnection of a single current half-wave is not taken into consideration.
10. Convective heat transfer from magneto-hydrodynamic effects is not taken into consideration.

3. Assumed forcing data

Electric forcing

For simulation's calculations following forcing data was assumed:

Current's waveform a sinusoidal current's half-wave of 50 Hz frequency.

[1)] As a matter of fact an anode receives about 10% more of an energy from an arc than a cathode [14]. For simulation simplification purposes only a single electrode was taken into consideration that is why the authors assumed equal division of the energy between the two electrodes and equal 50%. The authors' research on simultaneous simulation of anode and cathode receiving different energy will be the subject of further publications.

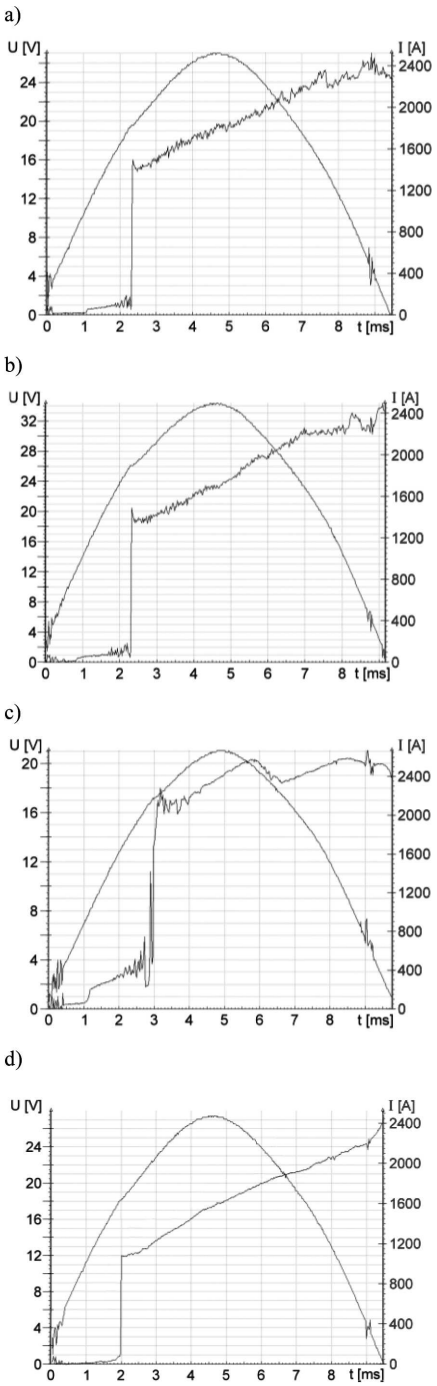

Fig. 3. Typical arc current and voltage waveforms a) Ag, b) Cu, c) W, d) Ag-W50

Current's amplitude 2,5; 4 and 7 kA.
Voltage source 500 V.
Arc's burning time 8 ms.
Arc-root's diameter 6 mm.
Contact's diameter 10 mm.

Figure 3 presents examples of typical current and arc voltage waveforms obtained for the test of tested contacts.

Thermal forcing

Three cases of arc's thermal power density at contacts surfaces were discussed:

Case A. Average thermal power density at the contact's surface is uniform and constant in time

It was assumed that arc-root's diameter and average thermal power density at the contact's surface, which is uniform, are constant during arc's burning time. It is the farthest reaching assumed simplification. This assumption is valid for DC currents. The calculations results will prove if such simplification can be used for AC currents.

For the forcing presented later in the paper it was assumed that electric arc starts to burn simultaneously on the area defined by the radius of arc-root on the contact's surface.

Tabulated values of the breaking arc's voltage waveform, current and power were done. Those are the values of typical registered waveforms in modelling research of contact material erosion properties [15-18].

Case B. Average thermal power density at the contact's surface is irregular, but constant in time

Average thermal power density in this case is irregular. Such case takes place in AC circuits. Along the arc-root's radius, thermal power density at the contact's surface decreases, as shown in Fig. 4. Such assumption is in line with considerations led by Bolanowski [24], Sobieszczuk [25] and Marusik [26].

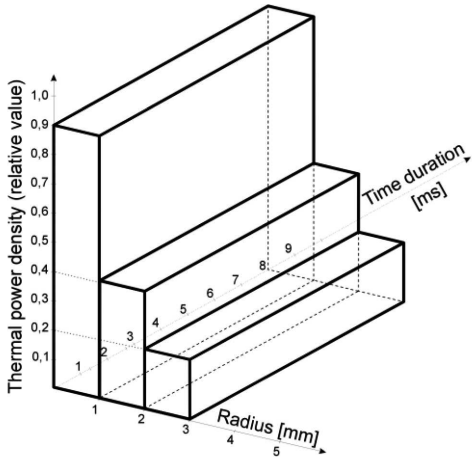

Fig. 4. Irregular thermal power density distribution in arc-root at the contact's surface

Case C. Thermal power density irregular at the contact's surface and in time

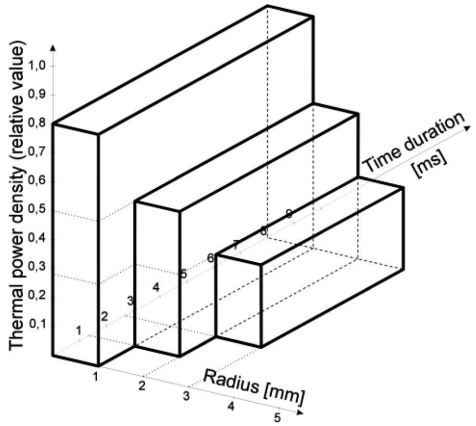

Fig. 5. Distribution of thermal power density irregular at the contact's surface and in time

In this case thermal forcing is the most similar in practice to AC circuits switches. The basis for such case are own observations results of the arc seen on pictures taken by fast

camera [27]. Change in arc-root diameter during the current's flow was visible on the film. Individual frames analysis allowed for the statement that power density is irregular at the whole arc-root's surface, what confirmed the earlier assumptions of Bolanowski [24]. On the Fig. 5 the irregularity in time of arc-root's radius and surface thermal power density distribution assumed for calculations was presented.

4. Calculations results

On the Fig. 6 the complete models of generated wireframes for 2D models are presented. The wireframe significantly affects the precision of the obtained results. The differences may reach hundreds of Celsius in degrees. Unfortunately, increasing the number of wireframe's elements significantly increases calculations time. In some important locations (contact overlays), in order to increase the calculations precision manual thickening of the wireframe was made. For example, the complete elements count was around 100 000, from which elements in contact overlay account for 85% and in contact base for 15%.

The numerical calculations precision is affected also by the number of steps, that is the number of timestamps, for which the application performs the calculations. Between these steps ANSYS averages the results. Thus, between the zero and the first step of the calculations space occurs what can be seen later on presented graphs of temperature as functions of time.

The preliminary simulation result for contact's temperature changes in function of time (made for Ag-W50 composite in case of thermal power density defined as case C) for calculated time equal to 250 ms was done. The shortening of calculation time to 45 ms may be allowed, because after this period temperatures in contact don't cause change in its physical state, therefore they don't lead to the degradation and destruction of contact's surface layer [28].

On the Fig. 7-11 sample simulation results for temperature field distribution in silver contacts for currents of 2,5 and 4 kA and in Ag-W50 composite for currents of 2,5, 4 and 7 kA were presented, for cases A, B, C of thermal power density distribution.

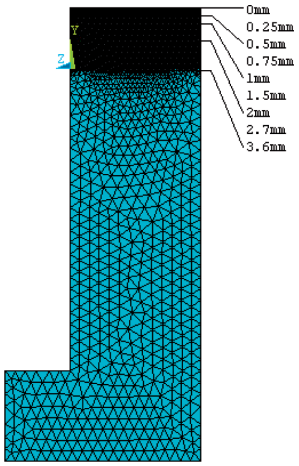

Fig. 6. Wireframe generated for 2D model, without boundary conditions

Fig. 8 presents a 3D distribution of temperature field for Ag contact, current's amplitude of 4 kA after: a) 9 ms, b) 45 ms. Fig. 9 presents a fragment of Ag contact's surface with temperature field distribution after removing components that have reached boiling point (a) – minimal mass loss (Δm = 164,9 mg) and melting point (b) – maximal mass loss (Δm = 562,8 mg); current's amplitude of 4 kA. Fig. 10 presents a fragment of Ag contact's surface with temperature field distribution after removing components that have reached boiling point (a) – minimal mass loss (Δm = 23,82 mg) and melting point (b) – maximal mass loss (Δm = 146,9 mg),

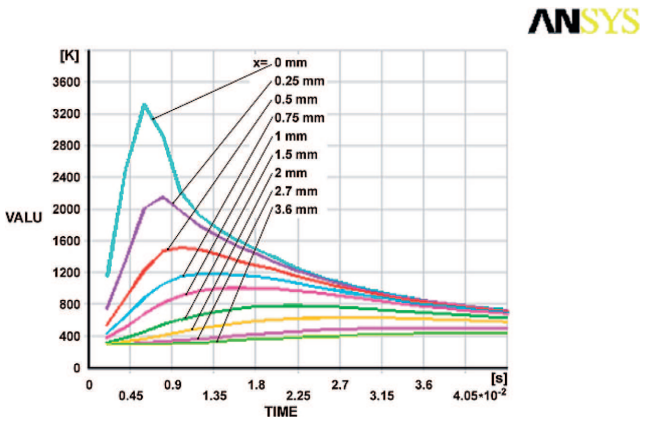

Fig. 7. Graph of temperature changes in time along contact's axis of symmetry (Fig. 6) for depths x = 0 – 3,6 mm, Ag contact, current's amplitude of 4 kA

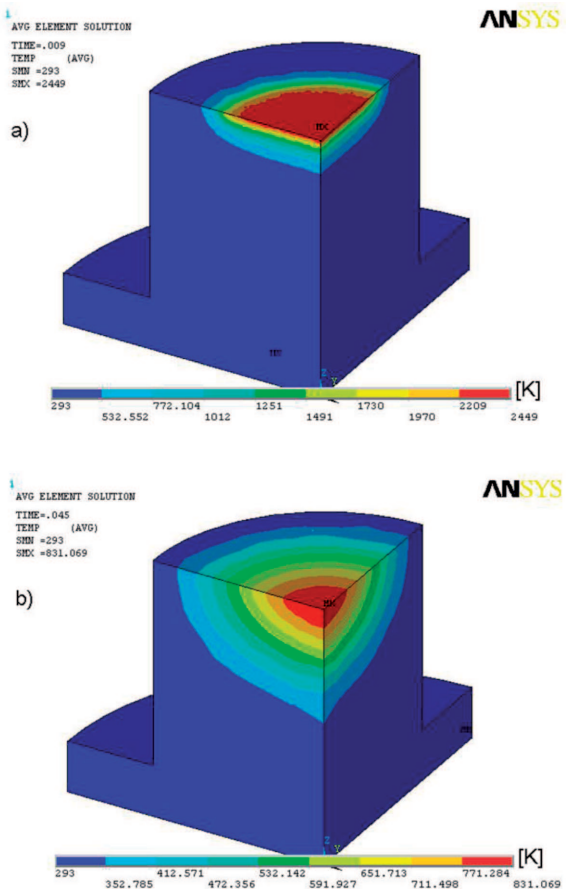

Fig. 8. 3D distribution of temperature field for Ag contact, current's amplitude of 4 kA after: a) 9 ms b) 45 ms

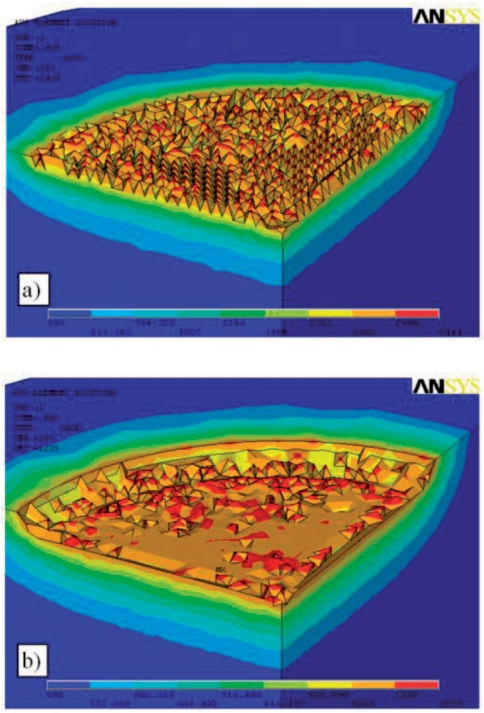

Fig. 9. Fragment of Ag contact's surface with temperature field distribution after removing components that have reached boiling point (a) – minimal mass loss (Δm = 164,9 mg) and melting point (b) – maximal mass loss (Δm = 562,8 mg); current's amplitude of 4 kA

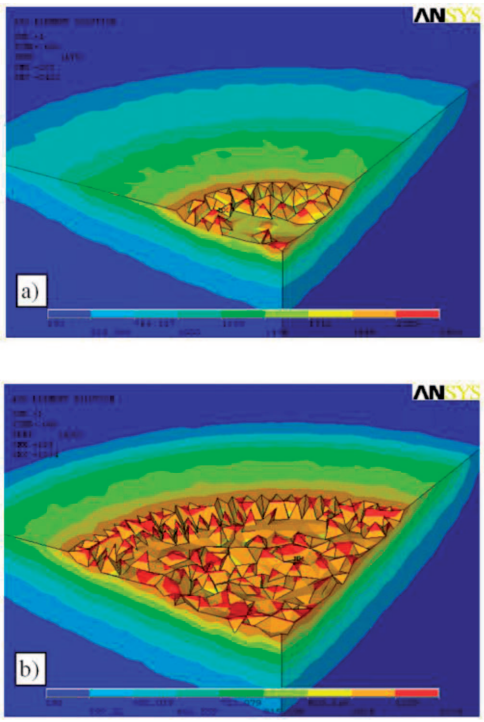

Fig. 10. Fragment of Ag contact's surface with temperature field distribution after removing components that have reached boiling point (a) – minimal mass loss (Δm = 23,82 mg) and melting point (b) – maximal mass loss (Δm = 146,9 mg), current's amplitude of 2,5 kA

current's amplitude of 2,5 kA. Fig. 11 presents a fragment of Ag contact's surface with temperature field distribution after removing components that have reached boiling point (a) – minimal mass loss (Δm = 23,35 mg) and melting point (b) – maximal mass loss (Δm = 159,6 mg); current's amplitude of 2,5 kA.

Additionally, the calculations for copper and tungsten contacts were conducted. Results of those simulations are not presented in the graphical form due to the limited size of this paper but only as tabulated values of ΔV volume and Δm mass loss (tables 1-3), what allows for formulating conclusions.

Simulation for thermal forcing case A (average thermal power density at the contact's surface is uniform and constant in time)

Simulation for thermal forcing case B (average thermal power density at the contact's surface is irregular but constant in time)

Simulation for thermal forcing case C (thermal power density is irregular at the contact's surface and in time)

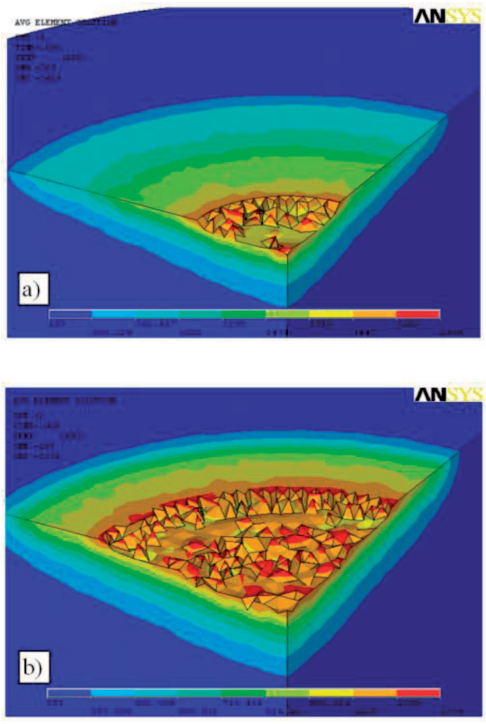

Fig. 11. Fragment of Ag contact's surface with temperature field distribution after removing components that have reached boiling point (a) – minimal mass loss (Δm = 23,35 mg) and melting point (b) – maximal mass loss (Δm = 159,6 mg); current's amplitude of 2,5 kA

5. Calculations results analysis and conclusions

In the ANSYS application four most commonly used materials for electric contacts production were used: copper, silver, tungsten and Ag-W50 composite. For each of these materials thermal forcing was used as different power density distribution. Thermal power density values were chosen that every analysed contact material would reach boiling and melting points, which usually happens at high current arc. It allows for estimating contact mass loss for those materials.

For the case A (p. 3), constant time and uniform thermal power density at the contact's surface, sinusoidal half-wave current amplitudes were as follow:

– for copper and silver – 4 kA,
– for tungsten and W–Ag50 composite – 4 and 7 kA.

For the two remaining forcing cases: irregular thermal power density at the contact's surface but constant in time (case B) and thermal power density irregular at the contact's surface and in time (case C) following current values were assumed:
– for copper and silver – 2,5 kA
– for tungsten and Ag–W50 composite – 2,5 and 4 kA.

Arc's thermal forcing lasting 8 ms in all cases, comprised about 60% of contact overlay's work surface.

For all the discussed forcing cases and contact materials the characteristic contact mass and volume losses were defined, according to erosion caused only by melting and evaporating (maximal value) or only by evaporating and removing of material by molecular diffusion (minimal value). Volume and mass of the removed material from the contact overlay for silver, copper and tungsten was calculated directly by using ANSYS application.

However for Ag-W50 composite contacts results were obtained by considering two theoretical cases.

Case 1, where only boiling state of a component of easily boiling composite was taken into consideration (silver) and it was assumed that mass loss is caused by removing from the contact's surface the fragment that reached evaporating point of easily melting component, while the hard melting component (tungsten) stayed in the solid state. Minimal contact mass loss is reached with these assumptions.

Case 2, where only melting state of a component of easily melting composite (silver) and the contact mass loss was defined as equal to removing from the contact's surface the fragment of silver volume that reached melting temperature. In this case maximal contact mass loss is reached. It was confirmed by the authors' research. A trap container [27] was used and a chemical analysis was carried out of the splashed trapped droplets. Chemical analysis by the means of atomics spectrometry method with inductively excited plasma ICP (Thermo Jarrell Ash, USA), showed that it consisted of 97,45%Ag, 0,95%W and others 1,6% (Si, C, Cu).

Obtained data is presented in tables 1-3.

Analysis of the obtained calculation results showed that in case of uniform thermal power density at the contact's surface and constant in time is significantly overestimating the dynamics of temperature distribution changes in the contact.

TABLE 1

Summary of material's volume and mass losses in case of maximal and minimal erosion (case A)

Material	Volume ΔV [mm³]				Mass Δm [mg]			
	Max. mass loss		Min. mass loss		Max. mass loss		Min. mass loss	
	4 kA	7 kA	4 kA	7 kA	4 kA	7 kA	4 kA	7 kA
Ag	53.60	–	15.7	–	562.8	–	164.90	–
Cu	48.48	–	6.67	–	436.4	–	59.72	–
W	5.59	37.38	–	12.76	107.8	721.6	–	246.40
Ag–W50	6.55	13.30	1.77	7.80	68.8	161.6	18.58	56.65

TABLE 2

Summary of material's volume and mass losses in case of maximal and minimal erosion (case B)

Material	Volume ΔV [mm³]				Mass Δm [mg]			
	Max. mass loss		Min. mass loss		Max. mass loss		Min. mass loss	
	2.5 kA	4 kA	2.5 kA	4 kA	2.5 kA	4 kA	2.5 kA	4 kA
Ag	13.98	–	2.27	–	146.90	–	23.82	–
Cu	10.83	–	1.20	–	97.52	–	10.75	–
W	0.96	4.50	–	1.10	18.57	86.16	–	21.25
Ag–W50	2.31	5.30	0.27	2.92	24.21	58.40	2.85	13.70

TABLE 3

Summary of material's volume and mass losses in case of maximal and minimal erosion (case C)

Material	Volume ΔV [mm³]				Mass Δm [mg]			
	Max. mass loss		Min. mass loss		Max. mass loss		Min. mass loss	
	2.5 kA	4 kA	2.5 kA	4 kA	2.5 kA	4 kA	2.5 kA	4 kA
Ag	15.20	–	2.224	–	159.60	–	23.35	–
Cu	12.16	–	1.114	–	109.50	–	10.03	–
W	1.056	4.465	–	0.98	20.38	87.24	–	18.92
Ag-W50	2.635	8.845	0.2825	4.72	27.7	121.2	2.96	15.40

TABLE 4

Summary of mass losses and material loss in depth for thermal power density distributed in arc-root irregularly but constant in time

Material	Mass Δm [mg]				Material loss depth Δh [mm]			
	Max. mass loss		Min. mass loss		Melting point T_t		Boiling point T_w	
	2.5 kA	4 kA	2.5 kA	4 kA	2.5 kA	4 kA	2.5 kA	4 kA
Ag	146.90	–	23.82	–	0.756	–	0.015	–
Cu	97.52	–	10.75	–	0.705	–	0.010	–
W	18.57	86.16	–	21.25	0.152	0.408	–	0.01
Ag–W50	24.21	58.40	2.85	13.70	–	–	–	–

As a result, values of contact mass losses are overestimated, even over 10 times. Therefore case A does not reflect real thermal-erosion processes occurring in the contact under effect of electric arc.

Real contact thermodynamic conditions under arc's effect are best reflected in case C, when thermal power density is irregular at the contact's surface and in time. In case C, the calculated maximal contact temperature (along contact's symmetry axis) in function of distance measured from the initial contact surface differs not much from the value calculated in case of irregular thermal power density at the contact's surface but constant in time (case B). In consequence values of mass loss for those two cases are close to each other. The difference between case B and C reaches up to 7% while between case A and C is at least three times higher.

Furthermore, the temperature characteristics in function of material loss depth due to erosion almost coincide in cases B and C. It may be concluded that thermal power density distribution, considered in case B, is precise enough for conducting calculations in ANSYS software. Additionally entering parameters of this distribution to ANSYS software is easier than for case C.

Significant for further considerations is knowledge of temperature distribution along the contact's axis in function of melted material's depth. Due to this, case B is sufficient for proper estimation of ranges of contacts erosion, following are given only dependencies for thermal power density distributed irregularly at the contact's surface, but constant in time. Calculations were made for t = 6 ms from the moment of arc's ignition (when the highest temperature occur). In Table 4 summaries of contact's mass losses and material losses in depth are presented.

When analysing the obtained temperature values the superiority of the composite material over metals can be noticed. The temperatures obtained with the same arc's current during simulation for the composite are almost always lower than the temperatures obtained for metals. It is due to thermal properties of those materials. Owing to this, depth of both material loss due to erosion and loss of volume of composite contact is lower. In consequence, the durability of composite material contact is greater than metal contact, which was confirmed by authors' and other scientists' research.

This proves that heat flow through composite material, which contains easily melting component and hard melting component, reduces the maximal temperatures values. According to the authors, it can be due to the phenomenon of reflecting heat from boundary surfaces of composite components. However, this issue is very difficult to calculate and in the accessible applications there are no such options. This issue requires additional research work.

6. Experimental verification

The authors also undertook an attempt to experimentally verify the calculations results. At the testing post described in [29-32] he conducted erosion research, registering with a fast camera short arc discharge dynamic for Ag, Cu, W, Ag-W50 materials and current of 2,5 kA and for W and Ag-W50 materials and current of 4 kA. All measurements were carried out for new contacts and in a single switching cycle. Measurements were conducted five times each on new contacts. All mass loss measurements results were presented as a mean value out of five measurements results. Ag-W50 contacts were made using manufacturing process involving filling a tungsten base with silver. Starting powder mix consisted of fine-grained tungsten powder (Fig. 12), tungsten trioxide (pores forming agent), nickelous nitrate (activation additive for sintering), silver oxide and polyvinyl alcohol (sliding agent), all in precisely determined proportions. Structure of the Ag-W composites prepared for testing is shown in Fig. 13. The obtained composites have fine-grained structure. No pores, cracks, separations have been found. Parameters of contacts under test: density 14,9 [g/cm^3] and hardness 59 [HRB].

Fig. 14-17 present photos of contact surfaces after the research and a video segment after t = 6 ms time from the moment of arc's ignition and in the Table 5 the results of measurements for mass losses for anode and cathode.

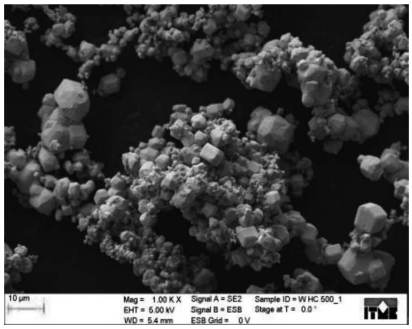

Fig. 12. Morphology of tungsten powder

Fig. 14 presents copper and silver contacts during a disconnection of 2.5 kA current. Since these materials have high

electrical conductivity and low temperature resistance there are clearly visible traces left by the removed melted material from the impact area of an arc root. Fig. 15a presents tungsten contact during disconnection of 2.5 kA current. There can be easily noticed an impact of a higher temperature on the anode surface than on the cathode surface. As a result, melted material is formed in a shape of wheel and it accumulates on the anode surface. On AgW50 contacts, after disconnection of 2.5 kA current (Fig. 15b), there is a visible trace made by an arc root with a typical, for this contact material, large border of silver melted out from the tungsten base. There can be also seen an exposed tungsten base deprived of silver filling what is confirmed by the visible porous structure. In case of disconnection higher current, 4 kA, there can be noticed similar traces left by an arc root but of greater size (Fig. 16).

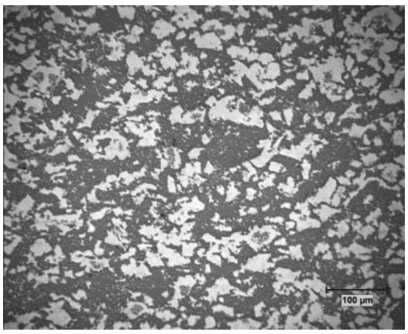

Fig. 13. Structures of W-Ag50 composites

TABLE 5

Measured mass losses for AG, CU, W, AG-W50

Material	Mass Δm [mg]			
	2.5 kA		4 kA	
	m_A [mg]	m_C [mg]	m_A [mg]	m_C [mg]
Ag	61.05	25.02	–	–
Cu	25.51	20.22	–	–
W	1.365	0.825	1.8	1.23
Ag-W50	3.08	1.97	10.65	6.78

By watching the fast camera video segments, and based on intensity of arc's lighting (Fig. 17), it can be concluded that with current's increase the temperature of metal drops leaving arc's area increases (Fig. 17e, f). Also visible is much greater number of metal drops around arc's column scattered to the surroundings (comparing Fig. 17d and Fig. 17f). Additionally size of the drops is significantly lower for arc's higher currents (Fig. 17f) which can be due to phenomenon of surface tension decrease strongly dependant on temperature.

It is also noticeable that arc diameter for t = 6 ms from the arc ignition moment (when, according to the calculations, the highest temperatures occur) is several times larger for 4 kA current (Fig. 17e, f) than for 2.5 kA current (Fig. 17a, d). Especially for 4kA current, it is clearly visible that plasma disc has been formed as a cathodal and anodal collision of a plasma flux. In the case of Ag-W50 composite, one can notice that for 4 kA current arc's root diameter equalled with contact diameter (Fig. 16a, b) and the characteristic melted silver crown (Fig. 15a, b) was removed by electro-dynamic forces in the arc's root outside the contact, what caused greater contact mass loss.

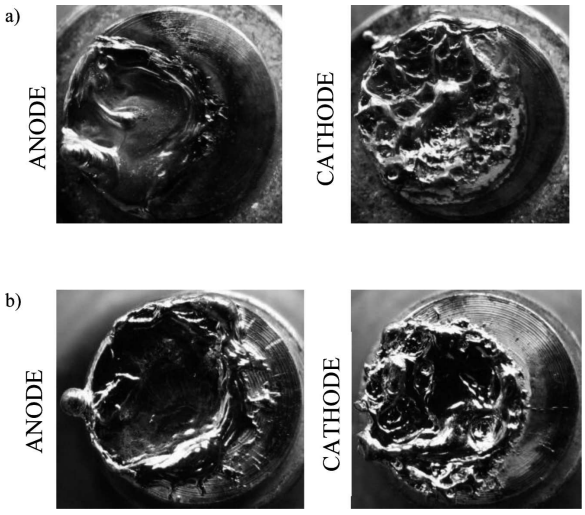

Fig. 14. Macrophotos of contact surfaces after turning off the 2.5 kA current: a) Cu-Q = 12.5 C, E = 306 J; b) Ag-Q = 12.7 C, E = 258 J

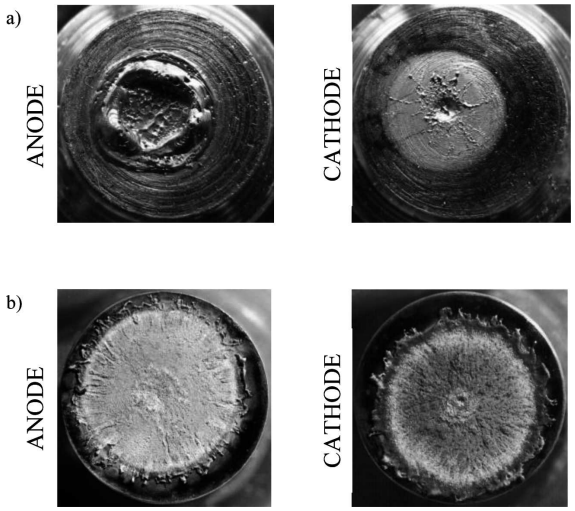

Fig. 15. Macrophotos of contacts surfaces after turning off the 2.5 kA current: a) W-Q = 13.6 C, E = 255 J; b) Ag-W50-Q = 13,7 C, E = 257 J

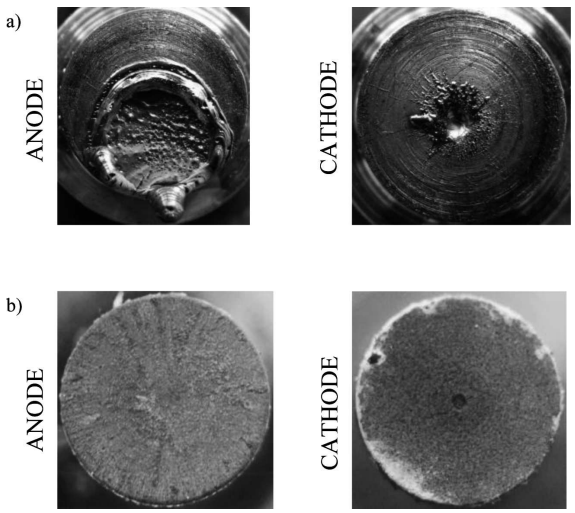

Fig. 16. Macrophotos of contacts surfaces after turning off the 4 kA current: a) W-Q = 20,4 C, E = 408 J; b) Ag-W50-Q = 23,2 C, E = 469 J

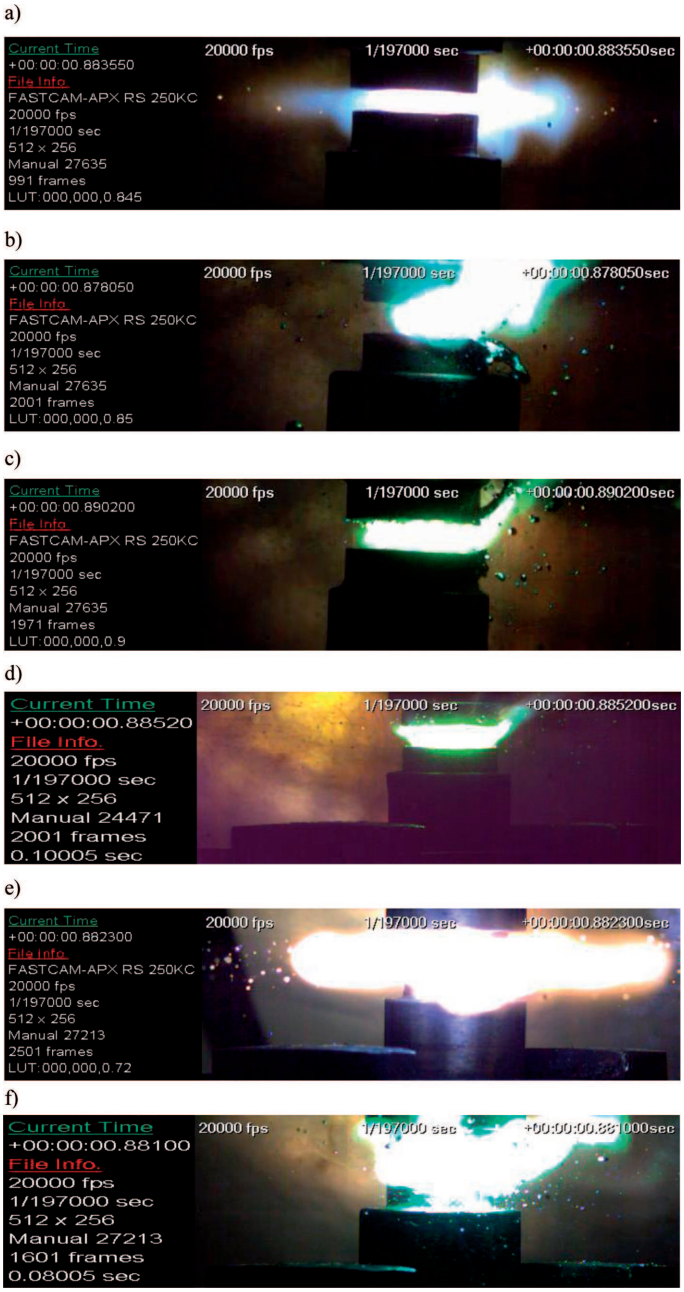

Fig. 17. Video segment from fast camera of arc discharge in the opening contact for time t = 6 ms. Speed of camera: 20.000 frames/s. Polarity: Upper – Anode, lower – Cathode: a) W – current's amplitude 2.5 kA d) Ag-W50 – current's amplitude 2.5 kA; b) Cu – current's amplitude 2.5 kA e) W – current's amplitude 4 kA; c) Ag – current's amplitude 2.5 kA f) Ag-W50 – current's amplitude 4 kA

7. Conclusions

The authors proposed a new approach to calculating contact mass loss using ANSYS software. For this purpose, he used the temperature field distribution analysis irregular in time and space and produced by contact's arc thermal forcing.

Basing on the conducted computer simulations, the following theoretical and practical conclusions can be formed:

1. Thermal power density distribution, irregular on contact's surface but constant in time, is precise enough for the ANSYS software to conduct the calculations of electric arc's thermal effect on the contact. Introducing the parameters of this distribution into ANSYS software is easier in this case than in case of thermal power density distribution that is irregular on the contacts surface and in time, although such case more precisely reflects real conditions of electric arc's burning.
2. Contact material loss obtained from the composite materials contacts simulation for the equal arc's current are almost always lower than the contact material loss obtained from pure easily-melting metal contacts (i.e. Ag, Cu). It is due to thermal properties of those materials. Because of this, material loss depth due to erosion and the composite contact's volume loss is lower. In consequence, the durability of composite materials contacts is greater than metal contacts, what was confirmed by the own results and those of other scientists research. This indicates that thermal flow through composite material, which contains easily-melting and hard-melting components, decreases the maximal temperatures values. According to the authors, it may be caused by the phenomenon of heat being reflected from the borderline surfaces of the composite's components. However, this issue is very hard to calculate and the applications that were available to the authors had no such capability. This issue requires additional scientific work.
3. The proposed modelling method of contact erosion using computer simulation, which allows for determining the minimal and maximal mass loss (Table II), is correct, because contact mass loss results obtained from experimental research (Table V) are included in the calculated ranges for mass loss. Thus, it will be possible to use this method in practice. Only tungsten mass loss deviates from calculated values and is lower. It is most probably due to fact that adhesion forces are big enough to not allow melted tungsten to separate from the contact surface and scatter to the surroundings. Those forces cause creation of towers and cones forming over the contact's surface even to 5 mm high (Fig. 14a and 15a) especially on the surface of tungsten anode. Real contact mass losses assume values closer to minimal mass losses which mainly includes material boiling, because it is hard to include in thermal calculations explosive discharge of the material to the surroundings, first by the thermodynamic dissolution of bridge and later by arc burning.

This paper is presented as the basis for more detailed elaborations, which will especially cover the subject of perfecting the technique of modelling the composite contacts materials and analysing the erosion phenomena without carrying out experiments.

REFERENCES

[1] T. Kubono, Contribution to the theory for the cathode erosion in the arc discharge. Proc. 8th ICECP, Tokyo, 198-202 (1976).
[2] I. Tchalakov, P. Petrov, Electric contacts heating as a result of the electric arc. Proc. 11th ITK, Berlin, 366-369 (1982).
[3] A. Lefort, P. Andanson, Experimental investigation of the energy exchange process at contacts subjected to an electic arc of intensity less than 3kA. Proc. 10th ICECP, Budapest, 129-137 (1980).

[4] A. Lefort, P. Andanson, R. Bessege, Energy transmitted to a metal contact by the cathode and anode of an electric arc. Proc. 33rd IEEE Holm Conference on Electrical Contacts, Chicago, 137-143 (1987).

[5] W. Bor-Jenq, S. Nannaji, Thermal analysis of electrode heating and melting due to a spark. Proc. 38th IEEE Holm Conference on Electrical Contacts, 51-63 (1992).

[6] E.I. Kim, S.N. Kharin et al., Thermophysical Processes in Electrical Contacts with Short Arc. Proc. 11th ICEC, Berlin, 82-85 (1982).

[7] J.P. Chabrerie, J. Devautour, Teste Ph.: A numerical model for thermal processes in an electrode submitted to an arc in air and its experimental verification. Proc. 38th IEEE Holm Conference on Electrical Contacts, Philadelphia, 1992, pp.65-70.

[8] Chabrerie J.P., Devautour J., Teste Ph.: A method for determination of the liquid and the vapor quantities created by an arc in air on contact electrodes: an original test device. Proc. 16th ICEC, Loughborough, 331-336 (1992).

[9] T.S. Davies, H. Nouri, M. Fairhurst, Experimental and theoretical study of heat transfer in switches. Proc. of 42th IEEE Holm Conference on Electrical Contacts, Chicago, 45-49 (1996).

[10] Y. Nakagawa, Y. Yoshioka, Theoretical calculation of the process of contact erosion using one dimensional contact model. Proc. 8th ICECP, Tokyo, 216-220 (1976).

[11] J. Swingler, J.W. McBride, Modeling of energy transport in arcing electrical contacts to determine mass loss. IEEE TCPM PART A **21**, 1, 54-60 (1998).

[12] F. Pons, M. Cherkaoui, An electrical arc erosion model valid for high current: Vaporization and Splash Erosion. Proc. 54th IEEE Holm Conference on Electrical Contacts, Orlando, OCT 27-29 2008, 9-14.

[13] P. Borkowski, Preliminary computer simulation of thermal influence of electric arc on contact during breaking of high current. Proc. 8th International Conference SAP&ETEP, Lodz, 237-241 (1997).

[14] P. Borkowski, E. Walczuk, Thermal Models of Short Arc between High Current Contacts. Proc. 47th IEEE Holm Conference on Electrical Contacts, Montreal, 259-264 (2001).

[15] P. Borkowski, Arc Erosion of Contacts on Switching High Current. Archives of Electrical Engineering, PAN in Warsaw **53**, 3, 259-287 (2004).

[16] P. Borkowski, Computer simulation of thermal processes in conducts and arc erosion of silver-tungsten composite materials. Proc. 10th International Conference SAP, Lodz, 96-101 (2005).

[17] P. Borkowski, Thermal Models of Short Arc for Contact Opening on an Half Cycle of High Current. Archives of Electrical Engineering, PAN in Warsaw **54**, 1, 109-122 (2005).

[18] P. Borkowski, Computer simulation of thermal processes in contacts and arc erosion of silver-tungsten composite materials. Archives of Electrical Engineering, PAN w W-wie **56**, 1, 89-98 (2007).

[19] B. Bolanowski, Balance of arc power low-voltage DC with a particular focus of cathode fall area. Doctor thesis, TU of Lodz (in polish), 1964.

[20] I. Barin, O. Knacke, Thermochemical properties of inorganic substances. Springer-Verlag Berlin Heidelberg New York Verlag Stahleisen m.b.H. Düsseldorf, 1973.

[21] David R. Lide, Handbook of chemistry and physics, CRC Press, Boca Raton, Florida, USA, 79th edition, 1998.

[22] Ch.D. Hodgman, Handbook of Chemistry and Physics, 40th edition, Chemical Rubber Publishing Co., Cleveland, Ohio 1959.

[23] R.C. Weast, et al eds., CRC Handbook of Chemistry and Physic. 70th Edition, CRC Press Inc., Boca Rotan, Florida, 1990.

[24] B. Bolanowski, Gęstość prądu w plamce katodowej oraz pole temperaturowe w katodzie łuku elektrycznego. Habilitation thesis, TU of Lodz (in polish), 1967.

[25] A. Sobieszczuk, Synteza zjawisk cieplnych na katodzie łuku elektrycznego w świetle aktualnego stanu badań nad wyładowaniami elementarnymi. Scientific work TU of Lublin (in polish), 146, 1985.

[26] M. Marusik, Dynamika wyładowania elementarnego łuku krótkiego. Doctor thesis, TU of Lodz (in polish), 1982.

[27] E. Walczuk, P. Borkowski, K. Frydman, D. Wojcik-Grzybek, W. Bucholc, M. Hasegawa, Migration of composite contact materials components at high current arcing. IEICE Transactions on Electronics **E90-C**, 7, 1377-1384 (2007).

[28] P. Borkowski, E. Walczuk, Influence of contact diameter no arc erosion of the polarized contacts at high current conditions. Proc. 10th International Conference SAP, Lodz, 111-115 (2005).

[29] P. Borkowski, D. Boczkowski, Computer-aided testing of contacts on switching high current. Archives of Electrical Engeneering, PAN in Warsaw **54**, 3, 253-263 (2005).

[30] P. Borkowski, D. Boczkowski, T. Wysocki, Computer-controlled system for testing contacts on switching high current. Measurement, ELSEVIER **40**, 3, 294-29 (2007).

[31] K. Frydman, D. Wojcik-Grzybek, P. Borkowski, The influence of the microstructure on the electrical properties of Ag-C, Ag-WC and Ag-W-C content materials. Archives of Metallurgy and Materials **58**, 4, 1059-1064 (2013).

[32] S. Księżarek, M. Woch, D. Kołacz, M. Kamińska, P. Borkowski, E. Walczuk, Progress in fabrication technology of silver-based contact materials with particular account of the Ag-Re and Ag-$SnO_2Bi_2O_3$ composites. Archives of Metallurgy and Materials **59**, 2, 501-508 (2014).

Received: 20 September 2014.